Spectral analysis of the magnetic Laplacian in the semiclassical limit

Jean-Philippe MIQUEU

PhD student at the Mathematics Research Institute of Rennes
Advisors : Monique DAUGE, Nicolas RAYMOND

February 2016

1. Introduction
   - Physical motivations
   - General problem
   - Literature on the semiclassical analysis of the magnetic Laplacian
   - Some articles on the topic
2. Spectral analysis of the magnetic Laplacian when $h \to 0$
   - Framework and notations
   - Heuristic about the rule of model operators
3. Numerical simulations (with the Finite Element Librairy Mélina++)
   - Bottom of the spectrum of the Pan and Kwek operator
   - Asymptotic of the first ten eigenvalues
   - First ten eigenmodes

Superconductivity

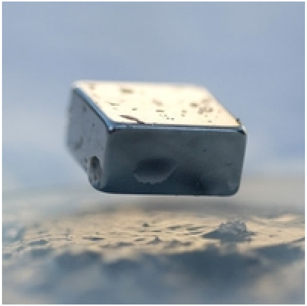

Magnetic Laplacian = Schrödinger operator with magnetic field

$$(-ih\nabla + \mathbf{A})^2 = \sum_{j=1}^{2}(hD_{x_j} + A_j)^2, \quad \boxed{D_{x_j} = -i\partial_{x_j}}$$

- h: the semiclassical parameter
- $\mathbf{A} = (A_1, A_2)$: the magnetic potential vector
- $\mathbf{B} = \nabla \times \mathbf{A}$: the magnetic field
- $(\lambda_n(h), \psi_{n,h})$: the eigenvalues and eigenfunctions

Magnetic Laplacian = Schrödinger operator with magnetic field

$$(-ih\nabla + \mathbf{A})^2 = \sum_{j=1}^{2} (hD_{x_j} + A_j)^2, \quad \boxed{D_{x_j} = -i\partial_{x_j}}$$

- h: the semiclassical parameter
- $\mathbf{A} = (A_1, A_2)$: the magnetic potential vector
- $\mathbf{B} = \nabla \times \mathbf{A}$: the magnetic field
- $(\lambda_n(h), \psi_{n,h})$: the eigenvalues and eigenfunctions

Question

$$(\lambda_n(h), \psi_{n,h}) \underset{h \to 0}{\sim} ?$$

Magnetic Laplacian = Schrödinger operator with magnetic field

$$(-ih\nabla + \mathbf{A})^2 = \sum_{j=1}^{2} (hD_{x_j} + A_j)^2, \quad \boxed{D_{x_j} = -i\partial_{x_j}}$$

- h: the semiclassical parameter
- $\mathbf{A} = (A_1, A_2)$: the magnetic potential vector
- $\mathbf{B} = \nabla \times \mathbf{A}$: the magnetic field
- $(\lambda_n(h), \psi_{n,h})$: the eigenvalues and eigenfunctions

Question

$$(\lambda_n(h), \psi_{n,h}) \underset{h \to 0}{\sim} ?$$

Bibliographic references

S. Fournais, B. Helffer, *Spectral methods in Surface Superconductivity*, Progress in Nonlinear Differential Equations and their Applications, 77, Birkhäuser Boston Inc., Boston, MA, 2010.

V. Bonnaillie-Noël, M. Dauge, N. Popoff, *Ground state energy of the magnetic Laplacian on corner domains*. To appear in Mémoires de la SMF, (2016).

N. Raymond, *Little Magnetic Book*. Preprint, 2016.

Some references with a non vanishing magnetic field:

Constant magnetic field $\mathbf{B} \equiv 1$:

- Bolley, Helffer (1997), Bauman-Phillips-Tang (1998), del Pino, Felmer, Sternberg (2000), (2D, disc),
- Helffer, Morame (2001), (2D, smooth boundary),
- Helffer, Morame (2004), (3D, smooth boundary),
- Bonnaillie (2005), (2D, corners),
- Fournais, Persson (2011), (3D, balls).

Non vanishing and variable magnetic field $\mathbf{B}$:

- Lu, Pan (1999) ; Raymond (2009) (2D, smooth boundary),
- Lu, Pan (2000) ; Raymond (2010) ; Helffer, Kordyukov (2013), (3D, smooth boundary),
- Bonnaillie-Noël (2005), Bonnaillie-Noël, Dauge (2006), Bonnaillie-Noël, Fournais (2007), (2D, corners).

Some references with a non vanishing magnetic field:

Constant magnetic field $\mathbf{B} \equiv 1$:

- Bolley, Helffer (1997), Bauman-Phillips-Tang (1998), del Pino, Felmer, Sternberg (2000), (2D, disc),
- Helffer, Morame (2001), (2D, smooth boundary),
- Helffer, Morame (2004), (3D, smooth boundary),
- Bonnaillie (2005), (2D, corners),
- Fournais, Persson (2011), (3D, balls).

Non vanishing and variable magnetic field $\mathbf{B}$:

- Lu, Pan (1999) ; Raymond (2009) (2D, smooth boundary),
- Lu, Pan (2000) ; Raymond (2010) ; Helffer, Kordyukov (2013), (3D, smooth boundary),
- Bonnaillie-Noël (2005), Bonnaillie-Noël, Dauge (2006), Bonnaillie-Noël, Fournais (2007), (2D, corners).

References with a vanishing magnetic field:

- Montgomery (1995), (the first case when the model of cancellation appears),
- Helffer, Morame (1996) (behaviour of the ground state in hypersurface),
- Pan, Kwek (2002), (2D, Neumann boundary condition),
- Helffer, Kordyukov (2009), (hypersurface),
- Dombrowski, Raymond (2013), (cancellation along a closed and smooth curve in the whole plane),
- Bonnaillie-Noël, Raymond (2015), (broken line of cancellation inside Ω, Neumann boundary condition),
- Attar, Helffer, Kachmar (2015), (minimizing of the energy when the Ginzburg-Landau parameter tends to infinity, Neumann boundary condition).

- $\Omega \subset \mathbb{R}^2$ open, bounded, simply connected, with smooth boundary
- $\mathbf{A} \in \mathcal{C}^\infty(\overline{\Omega}, \mathbb{R}^2)$
- Neumann magnetic boundary condition $(-ih\nabla + \mathbf{A})u \cdot \nu = 0$ on $\partial\Omega$

$$\mathrm{Dom}(\mathcal{P}_{h,\mathbf{A},\Omega}) = \{u \in H^2(\Omega), (-ih\nabla + \mathbf{A})u \cdot \nu = 0 \text{ on } \partial\Omega\}$$

$$\mathrm{Sp}(\mathcal{P}_{h,\mathbf{A},\Omega}) = \mathrm{Sp}_{\mathrm{disc}}(\mathcal{P}_{h,\mathbf{A},\Omega}) = (\lambda_n(h))_{n\in\mathbb{N}^*} = \{\lambda_1(h) \leq \lambda_2(h) \leq \cdots\}$$

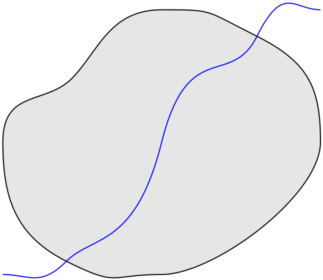

B vanishes along a smooth curve Γ

Assumptions:

- $\sharp(\Gamma \cap \partial\Omega) < \infty$ and Γ is non tangent to $\partial\Omega$
- $|\nabla\mathbf{B}(x)| \neq 0, \ \forall\, x \in \Gamma$

Localisation phenomena : concentration of the L^2 norm when $h \to 0$

$$g_1(x) = \frac{1}{\sqrt{h}} \exp\left(-\frac{|x|^2}{\sqrt{h}}\right), h = \frac{1}{5}$$

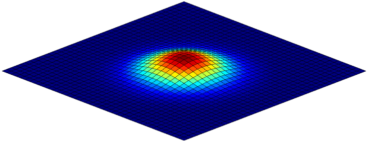

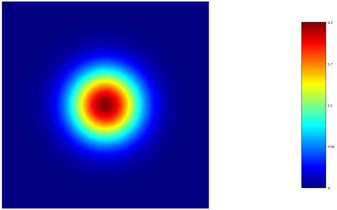

Localisation phenomena : concentration of the L^2 norm when $h \to 0$

$$g_1(x) = \frac{1}{\sqrt{h}} \exp\left(-\frac{|x|^2}{\sqrt{h}}\right), h = \frac{1}{10}$$

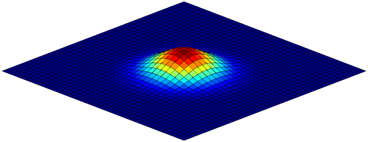

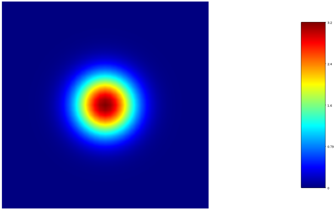

Localisation phenomena : concentration of the L^2 norm when $h \to 0$

$$g_1(x) = \frac{1}{\sqrt{h}} \exp\left(-\frac{|x|^2}{\sqrt{h}}\right), h = \frac{1}{20}$$

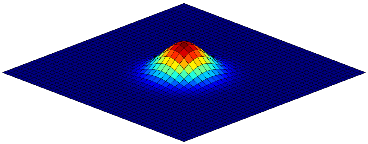

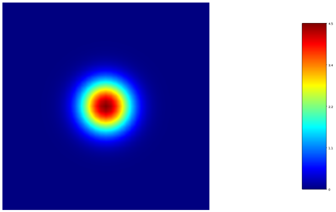

Localisation phenomena : concentration of the L^2 norm when $h \to 0$

$$g_1(\mathrm{x}) = \frac{1}{\sqrt{h}} \exp\left(-\frac{|\mathrm{x}|^2}{\sqrt{h}}\right), h = \frac{1}{40}$$

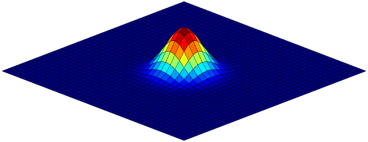

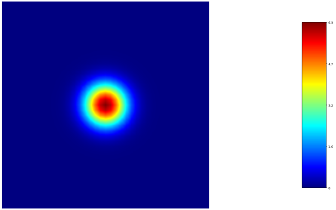

Localisation phenomena : concentration of the L^2 norm when $h \to 0$

$$g_1(x) = \frac{1}{\sqrt{h}} \exp\left(-\frac{|x|^2}{\sqrt{h}}\right), h = \frac{1}{80}$$

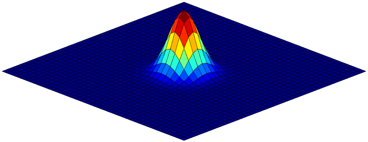

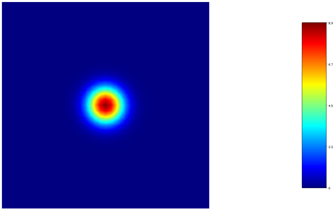

Where does the first eigenfunction(s) localize in the semiclassical limit?

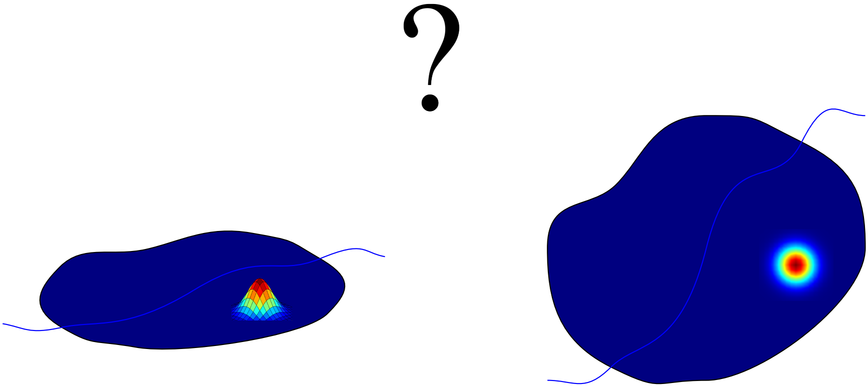

Different "areas" on Ω

1) $\boldsymbol{\Omega} \backslash (\partial\boldsymbol{\Omega} \cup \boldsymbol{\Gamma})$
2) $\partial\boldsymbol{\Omega} \backslash \boldsymbol{\Gamma}$
3) $\boldsymbol{\Gamma} \backslash \partial\boldsymbol{\Omega}$
4) $\partial\boldsymbol{\Omega} \cap \boldsymbol{\Gamma}$

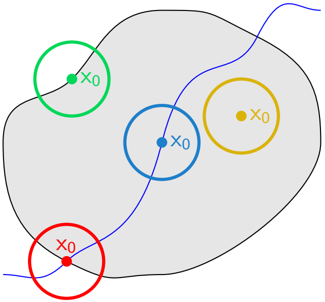

"Zoom" on each area

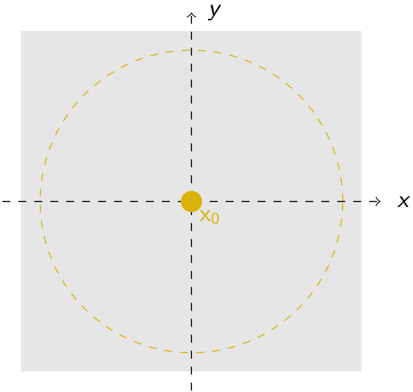

The magnetic Laplacian $\mathcal{P}_{1,\mathbf{A},\mathbb{R}^2}$ in the model case when $\mathbf{B} \equiv 1$:

$$D_y^2 + (D_x - y)^2$$

"Zoom" on each area

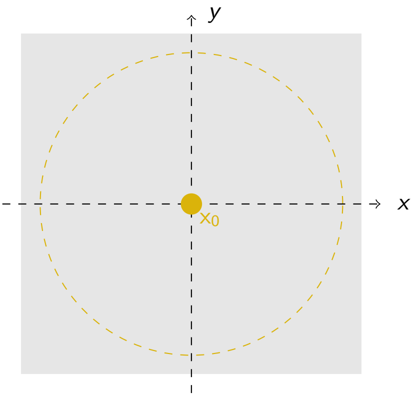

The magnetic Laplacian $\mathcal{P}_{1,\mathbf{A},\mathbb{R}^2}$ in the model case when $\mathbf{B} \equiv 1$:

$$D_y^2 + (D_x - y)^2$$

By unitary transforms, we are reduced to the harmonic oscillator:

$$\mathcal{H} = D_y^2 + y^2, \text{ on } \mathbb{R}$$

"Zoom" on each area

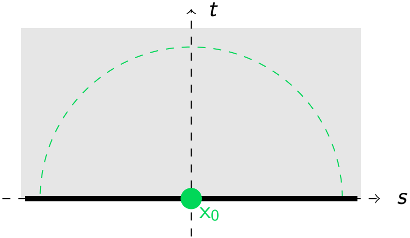

The magnetic Laplacian $\mathcal{P}_{1,\mathbf{A},\mathbb{R}^2_+}$ in the model case when $\mathbf{B} \equiv 1$:

$$D_t^2 + (D_s - t)^2$$

"Zoom" on each area

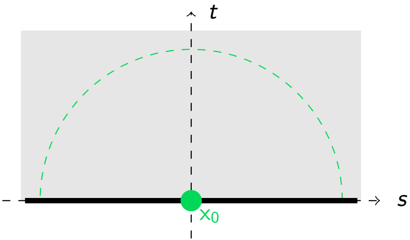

The magnetic Laplacian $\mathcal{P}_{1,\mathbf{A},\mathbb{R}^2_+}$ in the model case when $\mathbf{B} \equiv 1$:

$$D_t^2 + (D_s - t)^2$$

By unitary transforms, we are reduced to the De Gennes operator:

$$\mathcal{G}(\xi) = D_t^2 + (t - \xi)^2 \text{ on } \mathbb{R}_+ \text{ with Neuman boundary condition}$$

"Zoom" on each area

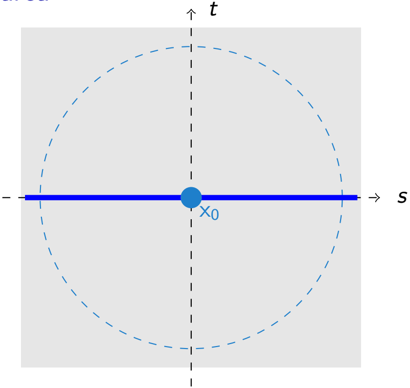

The magnetic Laplacian $\mathcal{P}_{1,\mathbf{A},\mathbb{R}^2}$ in the model case when $\mathbf{B}(s,t) = t$:

$$D_t^2 + \left(D_s - \frac{t^2}{2}\right)^2$$

"Zoom" on each area

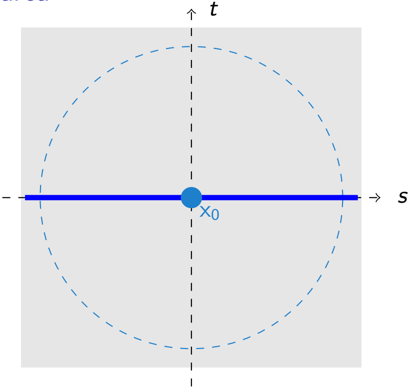

The magnetic Laplacian $\mathcal{P}_{1,\mathbf{A},\mathbb{R}^2}$ in the model case when $\mathbf{B}(s,t) = t$:

$$D_t^2 + \left(D_s - \frac{t^2}{2}\right)^2$$

By unitary transforms, we are reduced to the Montgomery operator:

$$\mathcal{M}(\eta) = D_t^2 + \left(\frac{t^2}{2} - \eta\right)^2 \text{ on } \mathbb{R}$$

"Zoom" on each area

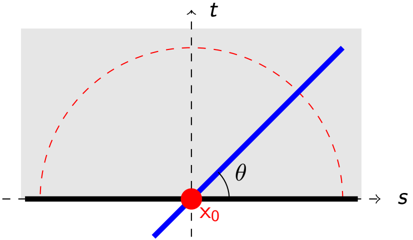

"Zoom" on each area

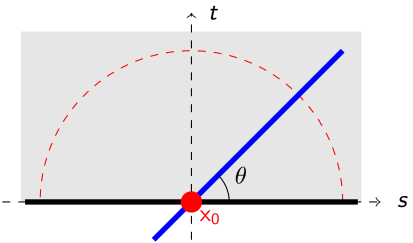

The magnetic Laplacian $\mathcal{P}_{1,\mathbf{A},\mathbb{R}^2_+}$ in the model case when $\mathbf{B}(s,t) = t\cos\theta - s\sin\theta$.
We get the Pan and Kwek operator:

$$\mathcal{K}_\theta = D_t^2 + \left(D_s + st\sin\theta - \frac{t^2}{2}\cos\theta\right)^2 \text{ on } \mathbb{R}^2_+$$

with Neumann boundary condition

Case	Operator of reference	Infimum of the spectrum
1	$\mathcal{H} = D_y^2 + y^2$ on $\mathbb{R}$	1
2	$\mathcal{G}(\xi) = D_t^2 + (t-\xi)^2$ on $\mathbb{R}_+$ with Neumann boundary condition	$\inf_{\xi\in\mathbb{R}} \mathrm{Sp}\,(\mathcal{G}(\xi)) = \Theta_0$
3	$\mathcal{M}(\eta) = D_t^2 + \left(\frac{t^2}{2} - \eta\right)^2$ on $\mathbb{R}$	$\inf_{\eta\in\mathbb{R}} \mathrm{Sp}\,(\mathcal{M}(\eta)) = \mathrm{M}_0$
4	$\mathcal{K}_\theta = D_t^2 + \left(D_s + st\sin\theta - \frac{t^2}{2}\cos\theta\right)^2$ on $\mathbb{R}_+^2$ with Neumann boundary condition	$\inf \mathrm{Sp}\,(\mathcal{K}_\theta) = \zeta_1^\theta$

Numerical computations:

- $\Theta_0 = \mu_1(\xi_0) \approx 0.5901$, with $\xi_0 = \sqrt{\Theta_0} \approx 0.7682$
- $\mathrm{M}_0 = \nu_1(\eta_0) \approx 0.5698$, with $\eta_0 \approx 0.35$

V. Bonnaillie-Noël, *Harmonic oscillators with Neumann condition of the half-line*, 2012.

V. Bonnaillie-Noël, N. Raymond, *Breaking a magnetic zero locus: model operators and numerical approach*, 2015.

The Pan and Kwek operator

$$\mathcal{K}_\theta = D_t^2 + \left(D_s + st\sin\theta - \frac{t^2}{2}\cos\theta\right)^2 \text{ on } \mathbb{R}^2_+ \text{ with Neumann boundary condition}$$

The Pan and Kwek operator

$$\mathcal{K}_\theta = D_t^2 + \left(D_s + st\sin\theta - \frac{t^2}{2}\cos\theta\right)^2 \text{ on } \mathbb{R}_+^2 \text{ with Neumann boundary condition}$$

Proposition:

$$\inf \mathrm{Sp}_{\mathrm{ess}}(\mathcal{K}_\theta) = \mathrm{M}_0$$

The Pan and Kwek operator

$$\mathcal{K}_\theta = D_t^2 + \left(D_s + st\sin\theta - \frac{t^2}{2}\cos\theta\right)^2 \text{ on } \mathbb{R}^2_+ \text{ with Neumann boundary condition}$$

Proposition:

$$\inf \mathrm{Sp}_{\mathrm{ess}}(\mathcal{K}_\theta) = \mathrm{M}_0$$

Proposition ([Pan-Kwek, 2002]):

- $\zeta_1^0 = \zeta_1^\pi = \mathrm{M}_0$
- $\zeta_1^\theta < \mathrm{M}_0$, for all $\theta \in (0, \pi)$

The Pan and Kwek operator

$$\mathcal{K}_\theta = D_t^2 + \left(D_s + st\sin\theta - \frac{t^2}{2}\cos\theta\right)^2 \text{ on } \mathbb{R}^2_+ \text{ with Neumann boundary condition}$$

Proposition:

$$\inf \mathrm{Sp}_{\mathrm{ess}}(\mathcal{K}_\theta) = \mathrm{M}_0$$

Proposition ([Pan-Kwek, 2002]):

- $\zeta_1^0 = \zeta_1^\pi = \mathrm{M}_0$
- $\zeta_1^\theta < \mathrm{M}_0$, for all $\theta \in (0, \pi)$

Proposition:

For all $\theta \in (0, \pi)$, ζ_1^θ is a eigenvalue and the associated eigenfunctions belong to $\mathscr{S}(\overline{\mathbb{R}^2_+})$.

Summary of the operator hierarchy

$x_0 \in \Omega \backslash (\partial\Omega \cup \Gamma), \partial\Omega \backslash \Gamma, \Gamma \backslash \partial\Omega, \partial\Omega \cap \Gamma$

Case	Operator h dependant	Infimum of the spectrum
1	$h^2 D_y^2 + (hD_y - \lvert\mathbf{B}(x_0)\rvert y)^2$ on $\mathbb{R}^2$	$\lvert\mathbf{B}(x_0)\rvert h$
2	$h^2 D_t^2 + (hD_s - \lvert\mathbf{B}(x_0)\rvert t)^2$ on $\mathbb{R}^2_+$ with Neumann boundary condition	$\Theta_0\lvert\mathbf{B}(x_0)\rvert h$
3	$h^2 D_t^2 + \left(hD_s - \lvert\nabla\mathbf{B}(x_0)\rvert \frac{t^2}{2}\right)^2$ on $\mathbb{R}^2$	$\mathrm{M}_0\lvert\nabla\mathbf{B}(x_0)\rvert^{\frac{2}{3}} h^{\frac{4}{3}}$
4	$h^2 D_t^2 + \left(hD_s + \lvert\nabla\mathbf{B}(x_0)\rvert \left(st\sin\theta(x_0) - \frac{t^2}{2}\cos\theta(x_0)\right)\right)^2$ on $\mathbb{R}^2_+$ with Neumann boundary condition	$\zeta_1^{\theta(x_0)}\lvert\nabla\mathbf{B}(x_0)\rvert^{\frac{2}{3}} h^{\frac{4}{3}}$

Approximation of the bottom of the spectrum of $\mathcal{P}_{h,\mathbf{A},\Omega}$

Theorem:

Under the condition

$$\inf_{x \in \partial\Omega \cap \Gamma} \zeta_1^{\theta(x)} |\nabla \mathbf{B}(x)|^{2/3} < \mathrm{M}_0 \inf_{x \in \Omega \cap \Gamma} |\nabla \mathbf{B}(x)|^{2/3}$$

we have two results:

1. **Asymptotique for the first eigenvalue**

$$\lambda_1(h) = h^{4/3} \inf_{x \in \partial\Omega \cap \Gamma} \zeta_1^{\theta(x)} |\nabla \mathbf{B}(x)|^{2/3} + \mathcal{O}(h^{5/3})$$

2. **Exponential concentration of the first eigenvector**

   There exist $C > 0$, $\alpha > 0$ and $h_0 > 0$, s. t. for all $h \in (0, h_0)$,

$$\int_\Omega e^{2\alpha h^{-1/3} d(x, \partial\Omega \cap \Gamma)} |\psi_{1,h}(x)|^2 \, dx \leq C \|\psi_{1,h}\|^2_{L^2(\Omega)}.$$

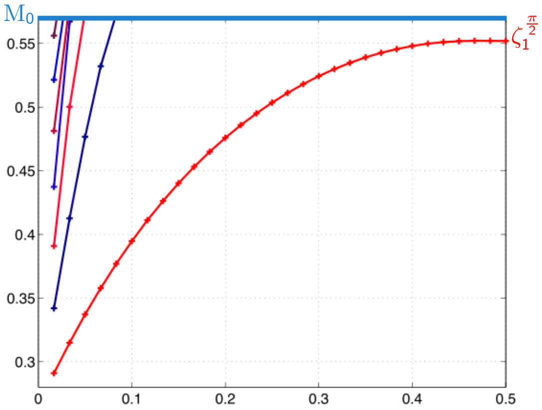

Figure : Eigenvalues ζ_n^θ below the bottom of the essential spectrum, for $\theta \in \{\frac{k\pi}{60}, 1 \leq k \leq 30\}$

Numerical computations:

- $\zeta_1^{\frac{\pi}{2}} \approx 0.5494$, $\mathrm{M}_0 \approx 0.5698$

V. Bonnaillie-Noël, N. Raymond, *Breaking a magnetic zero locus: model operators and numerical approach*, 2015.

$\mathbf{B}(s,t) = s$, $\Omega = [-\frac{3}{2}, \frac{3}{2}] \times [-1, 1]$

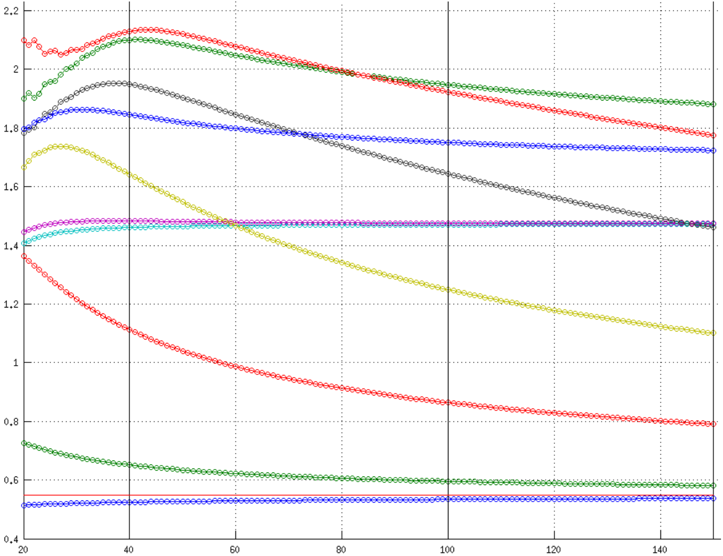

Figure : First ten eigenvalues $\lambda_n(h)$ rescaled by $h^{-4/3}$ according to $\frac{1}{h}$

$\psi_{n,h}$ (in modulus), $h = \frac{1}{40}$ with the numerical value of $\lambda_n(h)h^{-4/3}$

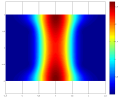
(1) 0.5243

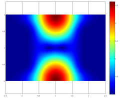
(2) 0.6515

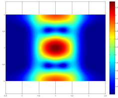
(3) 1.1119

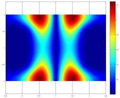
(4) 1.4610

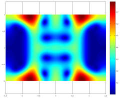
(5) 1.4827

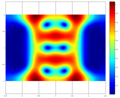
(6) 1.6416

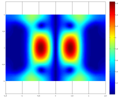
(7) 1.8452

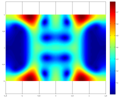
(8) 1.9485

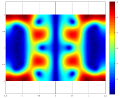
(9) 2.0997

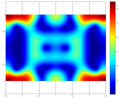
(10) 2.1300

Figure : Finite elements $\mathbb{P}_1$, 24×16 quadrangular elements of degree $\mathbb{Q}_{10}$

Y. Lafranche, D. Martin., *Melina++, bibliothèque de calculs éléments finis*, http://anum-maths.univ-rennes1.fr/melina/ (2012).

$\psi_{n,h}$ (in modulus), $h = \frac{1}{100}$ with the numerical value of $\lambda_n(h)h^{-4/3}$

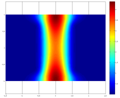

(1) 0.5337

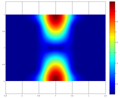

(2) 0.5956

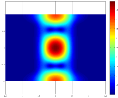

(3) 0.8638

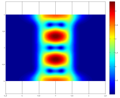

(4) 1.2487

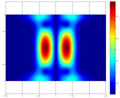

(5) 1.4704

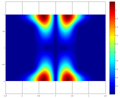

(6) 1.4753

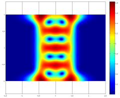

(7) 1.6437

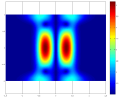

(8) 1.7504

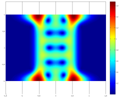

(9) 1.9231

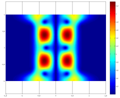

(10) 1.9472

Figure : Finite elements $\mathbb{P}_1$, 24×16 quadrangular elements of degree $\mathbb{Q}_{10}$

Y. Lafranche, D. Martin., *Melina++, bibliothèque de calculs éléments finis*, http://anum-maths.univ-rennes1.fr/melina/ (2012).

$\psi_{n,h}$ (in modulus), $h = \frac{1}{150}$ with the numerical value of $\lambda_n(h)h^{-4/3}$

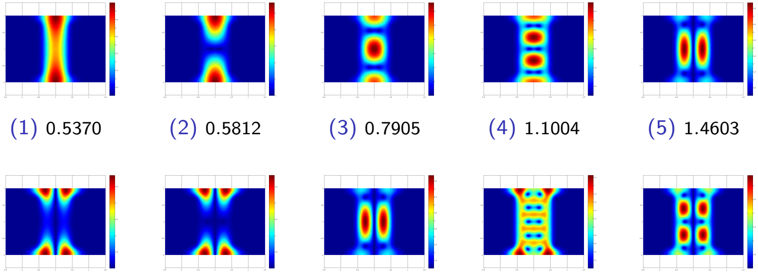

(1) 0.5370 (2) 0.5812 (3) 0.7905 (4) 1.1004 (5) 1.4603

(6) 1.4728 (7) 1.4750 (8) 1.7237 (9) 1.7738 (10) 1.8811

Figure : Finite elements $\mathbb{P}_1$, 24×16 quadrangular elements of degree $\mathbb{Q}_{10}$

Y. Lafranche, D. Martin., *Melina++, bibliothèque de calculs éléments finis*, http://anum-maths.univ-rennes1.fr/melina/ (2012).

Merci !

Argument of $\psi_{n,h}$, $h = \frac{1}{40}$ with the numerical value of $\lambda_n(h)h^{-4/3}$

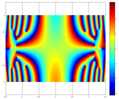

(1) 0.5243

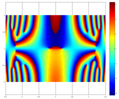

(2) 0.6515

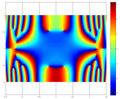

(3) 1.1119

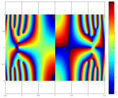

(4) 1.4610

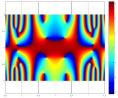

(5) 1.4827

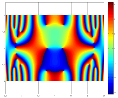

(6) 1.6416

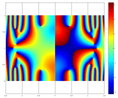

(7) 1.8452

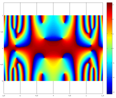

(8) 1.9485

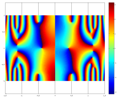

(9) 2.0997

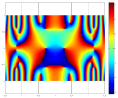

(10) 2.1300

Figure : Finite elements $\mathbb{P}_1$, 24×16 quadrangular elements of degree $\mathbb{Q}_{10}$

Y. Lafranche, D. Martin., *Melina++, bibliothèque de calculs éléments finis*, http://anum-maths.univ-rennes1.fr/melina/ (2012).

Argument of $\psi_{n,h}$, $h = \frac{1}{100}$ with the numerical value of $\lambda_n(h)h^{-4/3}$

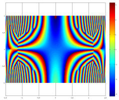

(1) 0.5337

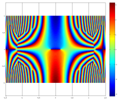

(2) 0.5956

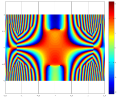

(3) 0.8638

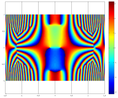

(4) 1.2487

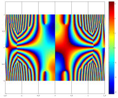

(5) 1.4704

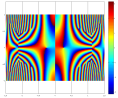

(6) 1.4753

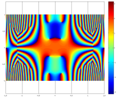

(7) 1.6437

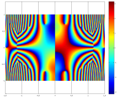

(8) 1.7504

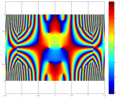

(9) 1.9231

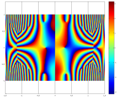

(10) 1.9472

Figure : Finite elements $\mathbb{P}_1$, 24×16 quadrangular elements of degree $\mathbb{Q}_{10}$

Y. Lafranche, D. Martin., *Melina++, bibliothèque de calculs éléments finis*, http://anum-maths.univ-rennes1.fr/melina/ (2012).

Argument of $\psi_{n,h}$, $h = \frac{1}{150}$ with the numerical value of $\lambda_n(h)h^{-4/3}$

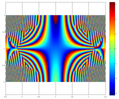
(1) 0.5370

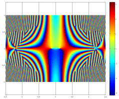
(2) 0.5812

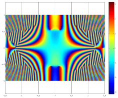
(3) 0.7905

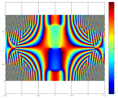
(4) 1.1004

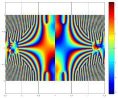
(5) 1.4603

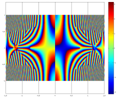
(6) 1.4728

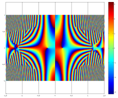
(7) 1.4750

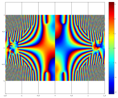
(8) 1.7237

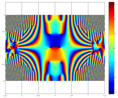
(9) 1.7738

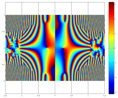
(10) 1.8811

Figure : Finite elements $\mathbb{P}_1$, 24×16 quadrangular elements of degree $\mathbb{Q}_{10}$

Y. Lafranche, D. Martin., *Melina++, bibliothèque de calculs éléments finis*, http://anum-maths.univ-rennes1.fr/melina/ (2012).